EPJ Web of Conferences **90**, 01003 (2015)
DOI: 10.1051/epjconf/20159001003

Particle production sources in pPb and PbPb at the LHC

Georg Wolschin[1,a]

[1] *Institut für Theoretische Physik der Universität Heidelberg, Philosophenweg 16, D-69120 Heidelberg, Germany, EU*

Abstract. Hadron production in relativistic heavy-ion collisions at LHC energies is investigated. After a brief consideration of stopping, particle production is accounted for in a nonequilibrium-statistical model with two fragmentation sources, and a central source that is mostly due to low-x gluon-gluon collisions. The particle content and energy dependence of the three sources is discussed for AuAu (RHIC) and PbPb (LHC). Results for asymmetric pPb collisions are compared with preliminary ALICE and ATLAS data.

1 Introduction

A brief survey of several features of hadron production in relativistic heavy-ion collisions at LHC energies is given in this article, which is essentially based on results published in [1], and obtained in [2, 3].

The stopping process in the very first phase of the collision is mostly characterized by the interaction of fast valence quarks with low-x gluons in the respective other nucleus. The fragmentation peaks in net-proton (proton – antiproton) rapidity distributions are clearly visible in SPS and RHIC data [4–7]. When considering rapidity or pseudorapidity distributions of produced charged particles, the fragmentation distributions also play a significant role, but since they shift to large values of rapidity at LHC, particle production near mid rapidity is almost exclusively determined by the central low-x gluon-gluon source.

This source cancels out in net-proton distributions, but in charged-hadron distributions its importance rises strongly with incident energy. In this note the relative importance of the three sources is investigated as function of energy from a direct comparison of the analytical solutions of a nonequilibrium-statistical relativistic diffusion model (RDM) [8] with PHOBOS [9] and recent ALICE data [10] data. This allows also for predictions at the LHC design energy, and for an analysis of the asymmetric pPb system at the current LHC energy of 5.02 TeV.

2 Stopping and fragmentation peaks

A QCD-based model that allows to calculate the two fragmentation peaks occurring at large values of the rapidity in net-baryon, or net-proton (proton minus antiproton) rapidity density distributions at and above SPS energies had been developed in [11, 12], and subsequent works, see fig. 1. It is found to be in good agreement with net-proton data from AuAu collisions at RHIC energies, but the position and magnitude of the predicted fragmentation peaks in PbPb collisions at LHC energies are presently beyond experimental reach due to the lack of particle identifcation beyond rapidities of about $|y| > 2$.

We have investigated both the mean rapidity loss $\langle \delta y \rangle$, and the fragmentation peak position y_{peak} as functions of the beam rapidity y_{beam} (or center-of-mass energy $\sqrt{s_{NN}}$). The peak position in $y-$space occurs somewhat below the beam rapidity. Already at a SPS energy of $\sqrt{s_{NN}} = 17.3$ GeV, the fragmentation peaks are clearly visible in the NA49 data [13], see fig. 1 [12]. They move further apart in rapidity space as the energy is increased to 62.4 GeV and 200 GeV at RHIC. At the maximum LHC energy of 5.52 TeV (y_{beam}=8.68), the fragmentation peaks are expected to be about 2 units of rapidity below the beam value according to the microscopic prediction, see [11].

Most of the physical processes leading to the rapidity loss in the peak region are of partonic nature: Fast valence quarks in the projectile collide with the gluon condensate in the respective other beam particle, thereby exchanging soft gluons, and reducing the beam energy and rapidity.

This behaviour in the peak region persists also at lower incident energies such as those reached at RHIC and SPS, and indeed one finds a linear dependence of the peak position (or the rapidity loss from y_{beam} to y_{peak}) on the beam rapidity [11] in agreement with the available data

$$y_{peak} = \frac{1}{1+\lambda}\left(y_{beam} - \ln A^{1/6}\right) + const \qquad (1)$$

for a saturation-scale exponent $\lambda = 0.2$, an empirical const=-0.2, and the mass number A. Here λ determines the Bjorken-x dependent value of the gluon saturation momentum $Q_s^2 = A^{1/3} Q_0^2 x^{-\lambda}$, with $Q_0^2 \simeq 0.04$ GeV^2 setting the momentum scale. The saturation-scale exponent $\lambda = 0.2$ corresponds to a gluon saturation momentum of $Q_s \simeq 0.77$ GeV at $x = 0.01$.

[a] e-mail: wolschin@uni-hd.de

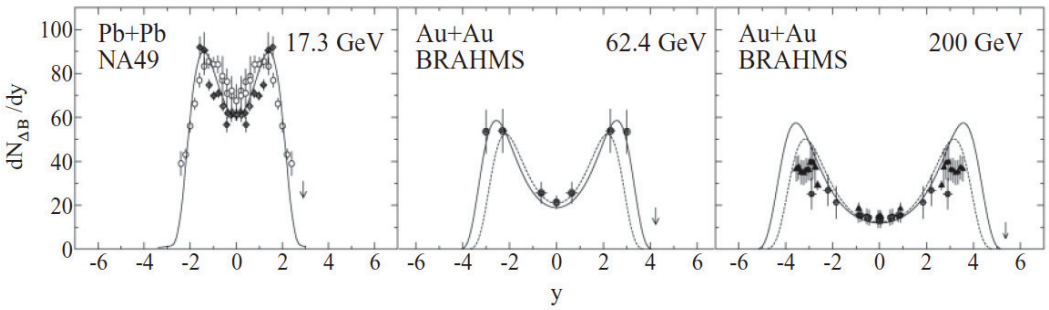

Figure 1. Calculated rapidity distribution of net baryons in a QCD-based approach to describe stopping in comparison with SPS and RHIC data. Central Pb + Pb collisions at SPS energies of $\sqrt{s_{NN}}$ = 17.3 GeV (left, NA49 data [13, 14]), and AuAu at RHIC energies of 62.4 GeV (middle), 200 GeV (right). BRAHMS data are from [4–7]. The theoretical fragmentation peak position depends weakly on the gluon saturation scale Q_s, see [12] for details. Theoretical distributions are shown here for values of the saturation-scale exponent λ = 0.2 (solid curves). Arrows indicate the beam rapidities. Dotted curves include the effect of a fragmentation function. From Mehtar-Tani and Wolschin [12].

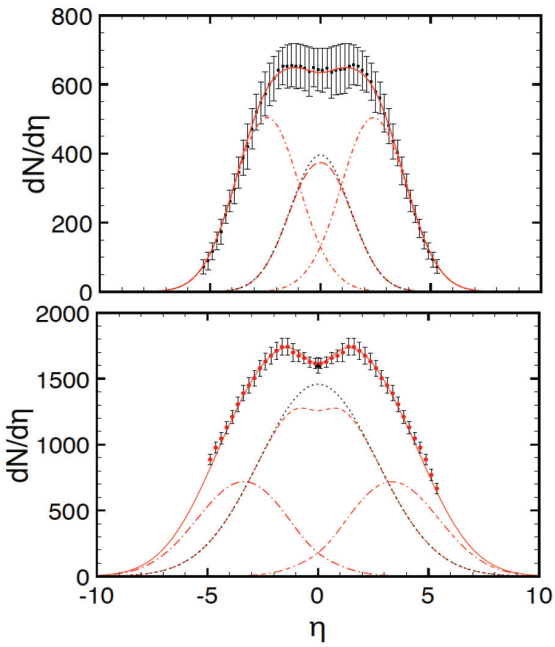

Figure 2. (Color online) The RDM pseudorapidity distribution functions for charged hadrons in central 200 GeV AuAu (top frame) and 2.76 TeV PbPb collisions are adjusted through χ^2−minimizations to the PHOBOS [9] (see also [15]) and ALICE [10] data, see [1]. The underlying particle production sources are shown: dash-dotted curves are the fragmentation sources, dashed curves the mid rapidity gluon-gluon sources, and dotted curves the central sources without the effect of the Jacobian transformation from rapidity to pseudorapidity. The particle content in the gluon-gluon source rises strongly with increasing c.m. energy. From [3]

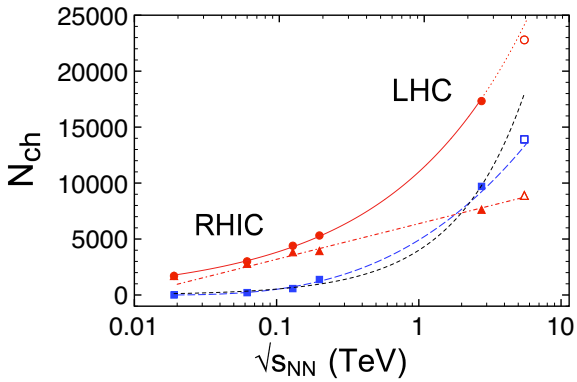

Figure 3. (Color online) Number of produced charged hadrons as function of the c.m. energy $\sqrt{s_{NN}}$ from RDM-fits of the available data for central heavy-ion collisions at 0.019, 0.062, 0.13, 0.2 TeV (RHIC, AuAu), 2.76 TeV (LHC, PbPb), plus extrapolation to 5.52 TeV. Circles are the total numbers, following a power law $\propto s_{NN}^{0.23}$. Triangles are particles from the fragmentation sources $\propto \log(s_{NN}/s_0)$. Squares are hadrons produced from the midrapidity source, with a dependence $\propto \log^3(s_{NN}/s_0)$. A power law $\propto s_{NN}^{0.44}$ [1] is also shown, but fails to fit the extrapolated 5.52 TeV yield. The gluon-gluon source (dashed) becomes the main source of particle production between RHIC and LHC energies. From [3].

3 Hadron production sources

The relativistic diffusion model (RDM) for the investigation of the time evolution of particle production sources in relativistic heavy-ion collisions has been applied in [1] to charged-hadron production in AuAu collisions at RHIC energies, and to PbPb collisions at LHC energies of 2.76 TeV. The sizes of the fragmentation sources, and of the mid rapidity gluon-gluon source have been identified as functions of centrality and energy. The results for central AuAu collisions at 200 GeV, and central PbPb collision at 2.76 TeV are shown in fig. 2, together with the underlying particle production sources.

The particle content in the low-x gluon-gluon source is seen to rise strongly with increasing c.m. energy, and constitutes the largest particle production source at LHC energies. The effect of the Jacobian transformation from rapid-

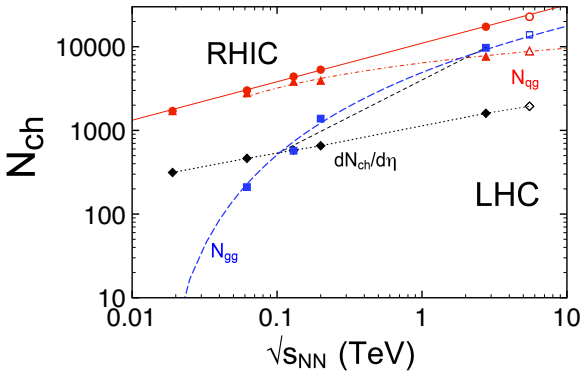

Figure 4. (Color online) The total charged-hadron production in central AuAu and PbPb collision in the energy region 19.6 GeV to 5.52 TeV is following a power law $N_{tot} \propto (s_{NN}/s_0)^{0.23}$ (solid line), whereas the particle content in the fragmentation sources is $Nqg \propto \ln(s_{NN}/s_0)$, dash-dotted curve. The particle content in the mid-rapidity source obeys $N_{gg} \propto \ln^3(s_{NN}/s_0)$, dashed curve, not too far from a power law (short-dashed line) only in the intermediate energy range 0.1–2.76 TeV. The energy dependence of the mid rapidity yield is shown as a dotted line. From [3].

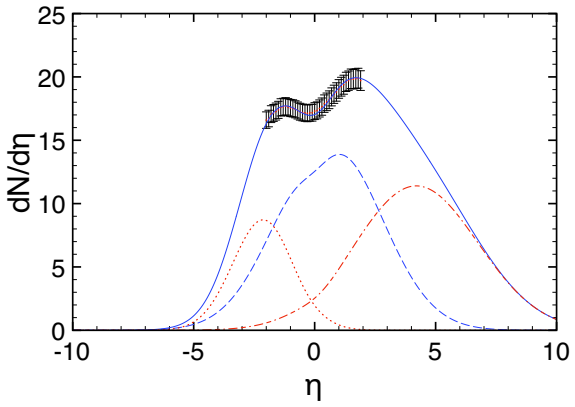

Figure 5. (Color online) The predicted RDM pseudorapidity distribution function for charged hadrons in minimum bias pPb collisions at LHC c.m. energy of 5.02 TeV shown here is adjusted in the mid-rapidity region to the ALICE data [16] (systematic error bars only). The underlying distributions in the three–sources RDM are also shown, with the dashed curve arising from gluon-gluon collisions, the dash-dotted curve from valence quark-gluon events in the Pb-like region, and the dotted curve correspondingly in the proton-like region. From [1].

ity y to pseudorapidity η – which acts mostly on the central source – is also shown. It causes a dip in the mid-rapidity source, but has a rather negligeable effect on the fragmentation sources at larger values of rapidity. The incoherent superposition of the sources gives a good representation of the ALICE data [10], and the five RDM parameters can be determined in a χ^2-minimization with respect to these data [1]. The minimum near mid rapidity occurs due to both, the effect of the Jacobian plus the interplay of fragmentation and central sources.

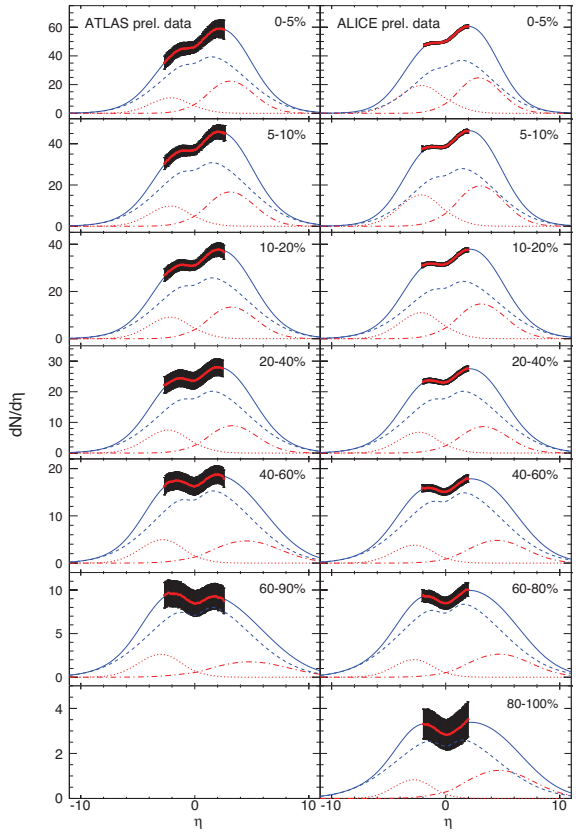

Figure 6. (Color online) The centrality-dependent RDM pseudorapidity distribution functions for charged hadrons in pPb collisions at LHC c.m. energy of 5.02 TeV are adjusted in the mid-rapidity region through χ^2–minimizations to the preliminary ATLAS (left) [17] and ALICE (right) [18] data (systematic error bars only for ALICE). The underlying distributions in the three–sources RDM are also shown, with the dashed curves arising from gluon-gluon collisions, the dash-dotted curves from valence quark-gluon events in the Pb-like region, and the dotted curves in the proton-like region (fragmentation sources). From [2].

The particle contents of the sources are displayed in Fig. 3, which resembles the analogous figure in [1], but differs in a decisive detail. The total particle content is found to follow a power law,

$$N_{ch}^{tot} = 1.1 \cdot 10^4 (s_{NN}/s_0)^{0.23} \tag{2}$$

with $s_0 = 1$ TeV^2, whereas the particle content in the two fragmentation sources is as expected a logarithmic function of the energy

$$N_{ch}^{qg} = 695 \cdot \ln(s_{NN}/s_0) \tag{3}$$

with $s_0 = 100$ GeV^2. The midrapidity gluon-gluon source is approximated by the thin dashed line following a power law as was already proposed in [1]

$$N_{ch}^{gg} \simeq 4 \cdot 10^3 (s_{NN}/s_0)^{0.44} \tag{4}$$

with $s_0 = 1$ TeV^2. However, when considering also the yield predicted within the relativistic diffusion model (RDM) for the LHC design energy of 5.52 TeV, the power

law fails to fit the expected yield, whereas a cubic log dependence agrees with the prediction,

$$N_{ch}^{gg} = 7.5 \cdot \ln^3(s_{NN}/s_0) \quad (5)$$

where s_0 =169 GeV^2.

It remains to be seen whether the data actually follow the model prediction. In the upcoming PbPb run at the LHC in 2015, the c.m. energy is scheduled to be 5.125 TeV, corresponding to 13 TeV pp. The total charged-hadron yield predicted by Eq. (2) at this energy is $N_{ch}^{tot} = 23,327$, with the central source contributing $N_{ch}^{gg} = 12,811$ charged hadrons according to Eq. (5).

When examining the RDM results for the particle content of the sources more closely also in the low-energy region where RHIC data are available, it turns out that the power law Eq. (4) is an acceptable approximation to N_{ch}^{gg} only between about 100 GeV and 2.76 TeV. This becomes particularly obvious in Fig. 4, where the same plot is shown using a double-logarithmic scale, following a suggestion by Trainor [19]. The cubic-log dependence of the gluon-gluon source (dashed) is seen to fit the points that have been extracted from my RDM-analyses [1] of PHOBOS and ALICE data rather precisely at the available energies, and it agrees with the RDM-prediction at the LHC design energy of 5.52 TeV.

As required by the RDM analysis of the 19.6 GeV AuAu data, the gluon-gluon contribution becomes unimportant below 20 GeV – whereas a power law would still predict a yield of about 100 charged hadrons per unit of rapidity in this energy region. Although a hybrid function with a log-dependence at RHIC energies that turns into a power law at LHC energies may appear as a reasonable compromise [20, 21], the $\ln^3$-dependence for the central source offers a more precise fit of the RDM-results. A more detailed discussion of this behaviour, and its underlying physical reason is given in [3].

4 Asymmetric systems

With the same approach, also asymmetric systems such as pPb at LHC energies can be investigated [1, 2]. Here the fragmentation sources have unequal particle content, and the midrapidity source is not centered at $\langle\eta\rangle = 0$, but at a centrality- and transverse momentum-dependent equilibrium value of the rapidity. The result for minimum-bias pPb collisions at the LHC energy of 5.02 TeV is shown [1] in fig. 5 in a χ^2-minimization with respect to ALICE data [16], and the centrality dependence [2] in comparison with preliminary ATLAS [17] and ALICE [18] data can be seen in fig. 6.

The RDM-analysis of pPb collisions at LHC energies reveals excellent agreement with the preliminary centrality-dependent data taken by both, the ALICE and the ATLAS collaborations. We have determined the RDM-parameters in χ^2- minimizations with respect to these data. At all centralities, the mid-rapidity source has the largest particle content, but the fragmentation sources are necessary for a detailed understanding of the centrality-dependent shape of the total distribution functions. It is the interplay of the three sub-distributions together with the effect of the Jacobian transformation that determines the pseudorapidity density distribution of produced charged hadrons.

The shapes of the total distribution functions indicate that the system has not reached statistical equilibrium. In particular, the centres of the fragmentation distributions remain far from the equilibrium values $y_{eq}(b)$: It is not just the produced-particle yields that determine whether the emitting source is in statistical equilibrium, but rather the shapes of the distribution functions, which clearly deviate from equilibrium distributions – although local equilibrium in the hydrodynamic sense appears to be achieved for events with $p_T \leq 6 - 8$ GeV/c as may be inferred from the success of hydrodynamics to describe bulk properties.

5 Conclusion

Particle production sources in relativistic heavy-ion collisions at RHIC and LHC energies and their energy dependence have been investigated. The relevance and effect of the fragmentation sources not only in stopping, but also in particle production has been outlined, and discussed as function of incident energy.

The particle content in the mid-rapidity low-x gluon-gluon source increases rapidly (stronger than a power law) with incident c.m. energy, and becomes larger than the content of the fragmentation sources between RHIC and LHC energies. Charged-hadron production in the asymmetric pPb system at 5.02 TeV and its centrality and energy dependence has been discussed accordingly.

Acknowledgements

I am grateful to the organizers of ISMD2014 – in particular, Fabrizio Fabbri and Paolo Giacomelli – for setting up this interesting conference in the splendid Oratory of San Filippo Neri in Bologna, and to Tom Trainor for his suggestions related to the topic of this article.

References

[1] G. Wolschin, J. Phys. G: Nuclear and Particle Physics **40**, 45104 (2013)

[2] P. Schulz, G. Wolschin, submitted to J. Phys. G: Nuclear and Particle Physics (2014)

[3] G. Wolschin, submitted to Phys. Rev. C (2014)

[4] I.G. Bearden *et al.* (BRAHMS Collaboration), Phys. Rev. Lett. **93**, 102301 (2004)

[5] H.H. Dalsgaard *et al.* (BRAHMS Collaboration), Int. J. Mod. Phys. E **16**, 1813 (2007)

[6] R. Debbie *et al.* (BRAHMS Collaboration), J. Phys. G **35**, 104004 (2008)

[7] I.C. Arsene *et al.* (BRAHMS Collaboration), Phys. Lett. B **677**, 267 (2009)

[8] G. Wolschin, Phys. Rev. C **69**, 024906 (2004)

[9] B. Alver et al. (PHOBOS Collaboration), Phys. Rev. C **83**, 024913 (2011)

[10] M. Guilbaud et al. (ALICE Collaboration), Nucl. Phys. A **904**, 381c (2013)

[11] Y. Mehtar-Tani, G. Wolschin, Phys. Rev. Lett. **102**, 182301 (2009)

[12] Y. Mehtar-Tani, G. Wolschin, Phys. Rev. C **80**, 054905 (2009)

[13] H. Appelshäuser *et al.* (NA49 Collaboration), Phys. Rev. Lett. **82**, 2471 (1999)

[14] C. Blume *et al.* (NA49 Collaboration), PoS (Confinement) **8**, 110 (2008)

[15] G. Wolschin, M. Biyajima, T. Mizoguchi, N. Suzuki, Annalen Phys. **15**, 369 (2006)

[16] B. Abelev et al. (ALICE Collaboration), Phys. Rev. Lett. **110**, 032301 (2013)

[17] B. Cole et al. (ATLAS Collaboration), ATLAS-CONF-2013-096 p. to be published (2013)

[18] A. Toia et al. (ALICE Collaboration), Proc. Quark Matter Conf. p. in press (2014)

[19] T. Trainor, priv. comm. (2014)

[20] R. Sahoo, A. Mishra, Int. J. Mod. Phys. E **23**, 1450024 (2014)

[21] R. Sahoo, A. Mishra, N. Behera, B. Nandi, submitted to AHEP, and arXiv:1408.5773 (2014)